THE JOURNAL OF PHYSICAL CHEMISTRY A

ARTICLE

pubs.acs.org/JPCA

State-to-State Quantum Dynamics Calculations of the C + OH Reaction on the Second Excited Potential Energy Surface

M. Jorfi

LOMC, FRE 3102 CNRS/Université du Havre, 76058 Le Havre Cedex, France

P. Honvault*

Laboratoire Interdisciplinaire Carnot de Bourgogne, UMR CNRS 5209, Université de Bourgogne, 21078 Dijon Cedex, France
Institut UTINAM, UMR 6213 CNRS, Université de Franche-Comté, 25030 Besançon Cedex, France

ABSTRACT: Accurate three-dimensional quantum-mechanical scattering calculations using a time-indepedent hyperspherical method have been performed for the $C(^3P) + OH(X^2\Pi) \rightarrow CO(a^3\Pi) + H(^2S)$ reaction on the second excited potential energy surface of $1^4A''$ symmetry. State-to-state reaction probabilities at a total angular momentum $J = 0$ have been computed in a wide range of collision energies. Many pronounced resonances have been found, espcially at low energy. The product vibrational distributions are noninverted. The present results therefore suggest that the title reaction proceeds via a long-lived intermediate complex. An approximate quantum-mechanical rate constant has also been calculated, and large differences are observed with the quasi-classical trajectory prediction.

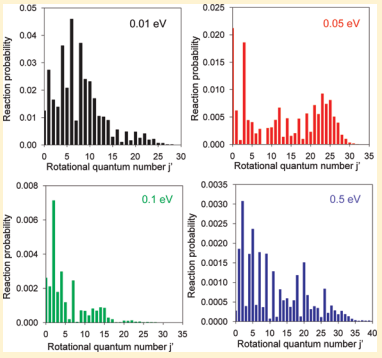

I. INTRODUCTION

In 2006, we built a global potential energy surface (PES) on the ground X^2A' state of HCO.[1] Then, quasi-classical trajectory (QCT)[2−4] and time-dependent wave packet (TDWP)[5,6] scattering calculations have been performed on this PES for the $C(^3P) + OH(X^2\Pi) \rightarrow CO(X^1\Sigma^+) + H(^2S)$ reaction. The results determine that the reaction occurs through a direct mechanism. Indeed, although the ground PES presents a large well depth (7.3 eV relative to the entrance channel), the triatomic intermediate complex is very-short-lived. Recently, our group has generated analytical global PESs for the first ($1^2A''$) and second ($1^4A''$) electronic states[4] using the "Reproducing Kernel Hilbert Space" method.[1,7] Ab initio calculations were performed at the multireference internally contracted single and double configuration interaction level plus Davidson correction. The two PESs correlate to the same entrance channel as the ground PES, while the $CO(a^3\Pi) + H(^2S)$ product exit channel involved CO in its first excited electronic state. Zanchet et al.[4] performed QCT calculations to obtain the thermal rate constants on each of the three adiabatic electronic states, X^2A', $1^2A''$, and $1^4A''$. The two other $2^2A'$ and $1^4A'$ states, which correlate to the $C(^3P) + OH(X^2\Pi)$ entrance channel and the $CO(a^3\Pi) + H(^2S)$ product channel, are energetically not favorable to the reaction. The $2^2A'$ state has a potential barrier of 0.2 eV in the entrance channel, and the reaction is therefore endothermic on this state at low collision energy. The $1^4A'$ state presents long-range potential wells and repulsive wall for carbon approaches near OH. No global PESs have therefore been computed for these states. Figure 1 shows schematic energy diagrams for the C + OH reaction on the three lowest electronic states. More details about the HCO PESs can be found in refs 1 and 4.

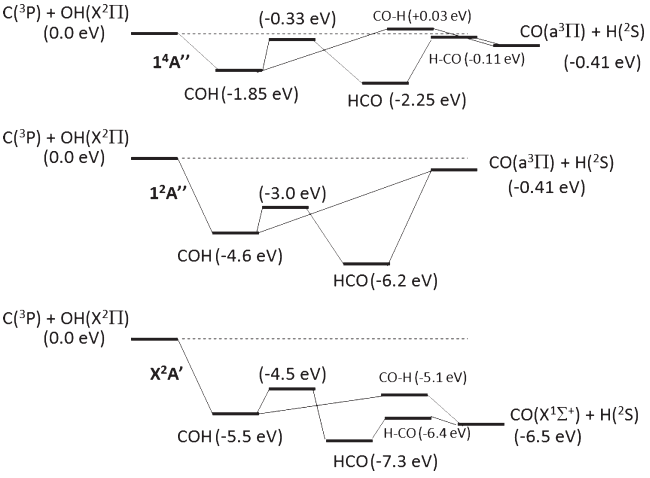

Figure 1. Schematic potential energy profiles for the C + OH system.

The quantum-mechanical (QM) study of the $C(^3P) + OH(X^2\Pi) \rightarrow CO(a^3\Pi) + H(^2S)$ reaction is very challenging

Received: March 28, 2011
Revised: July 1, 2011
Published: July 16, 2011

dx.doi.org/10.1021/jp202879n | J. Phys. Chem. A 2011, 115, 8791–8796

because it involves three different atoms: two heavy atoms (C and O) and a deep potential well. Very recently, we performed the first state-to-state QM calculations[8] for this reaction on the $1^2A''$ first excited state using a time-independent QM (TIQM) method. Reaction probabilities and rovibrational distributions of CO were determined for a total angular momentum $J = 0$.

In the present work, we are interested in the reaction dynamics on the $1^4A''$ PES. This PES is characterized by some similarities with the ground PES, such as the number of extrema. However, the exoergicity (without the zero-point energies) of the C + OH reaction is −6.5 eV on the ground PES and only −0.41 eV on the $1^4A''$ state. The title reaction is barrierless for angles of carbon approaches around $\theta = 70°$, while it presents a large barrier for linear (or nearly) geometries. The direct reaction mechanism via COH at low collision energy is therefore not favored, and the reaction proceeds rather via an indirect insertion mechanism involving the HCO intermediate. The global minimum is found for the HCO conformation with an energy of 2.25 eV below the $C(^3P) + OH(X^2\Pi)$ asymptote. The COH conformation corresponds to a second minimum at −1.85 eV relative to entrance channel. The first saddle point corresponds to the H−CO dissociation, and has an energy of −0.11 eV relative to the entrance channel. The second saddle point is associated with the CO−H dissociation and is located at 0.03 eV above the entrance channel. Thus, at collision energies below 0.03 eV, the CO−H dissociation cannot classically occur, while the H−CO dissociation is still possible. The third saddle point corresponds to the HCO/COH isomerization barrier located at −0.33 eV relative to C + OH. The isomerization therefore occurs at all collision energies. In conclusion, the features of the $1^4A''$ PES show that the reaction preferentially proceeds through the global minimum HCO. More details about the $1^4A''$ can be found in ref 4.

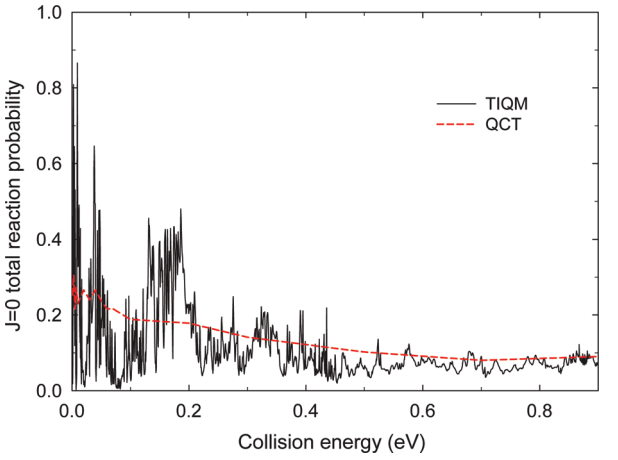

Figure 2. TIQM (solid line) and QCT (dashed line) $J = 0$ total reaction probabilities as a function of the collision energy for the C + OH($v = 0$, $j = 0$) → CO($a^3\Pi$) + H reaction.

The TIQM method has been used to investigate at the state-to-state level the dynamics of the C + OH reaction on the $1^4A''$ second excited electronic state. Vibrationally and rotationally product state-resolved reaction probabilities have been computed

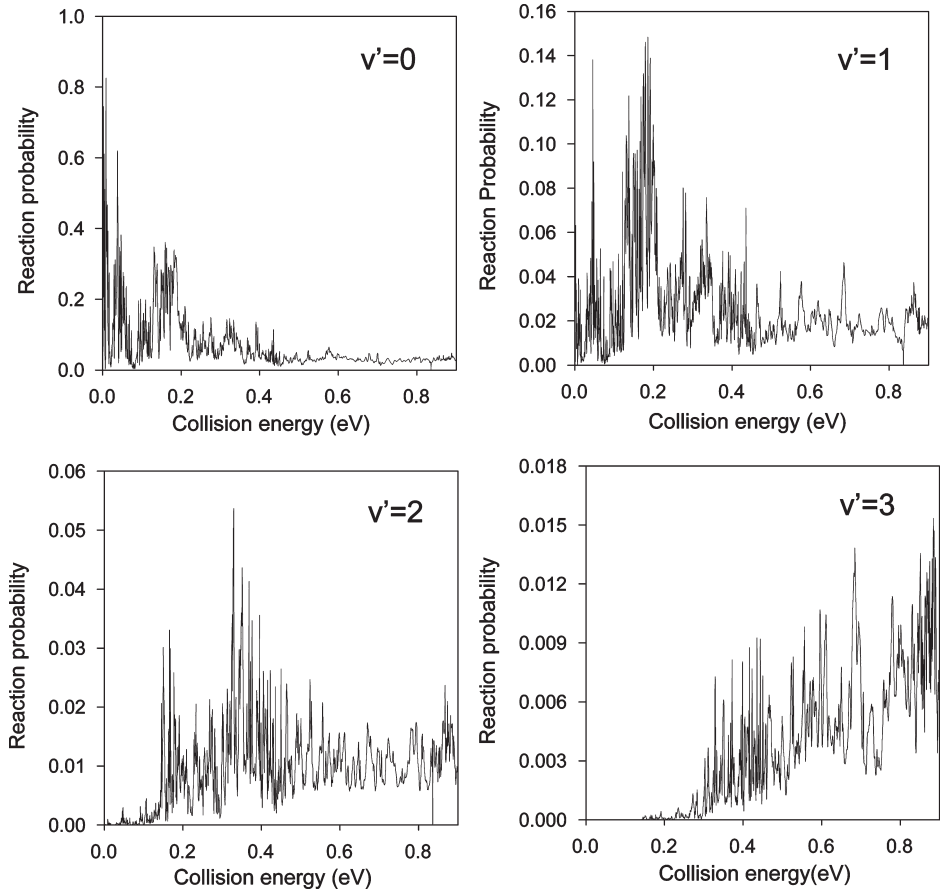

Figure 3. Vibrationally state-resolved probabilities as a function of the collision energy for the C + OH($v = 0$, $j = 0$) → CO($a^3\Pi$)(v') + H reaction at $J = 0$.

dx.doi.org/10.1021/jp202879n |J. Phys. Chem. A 2011, 115, 8791–8796

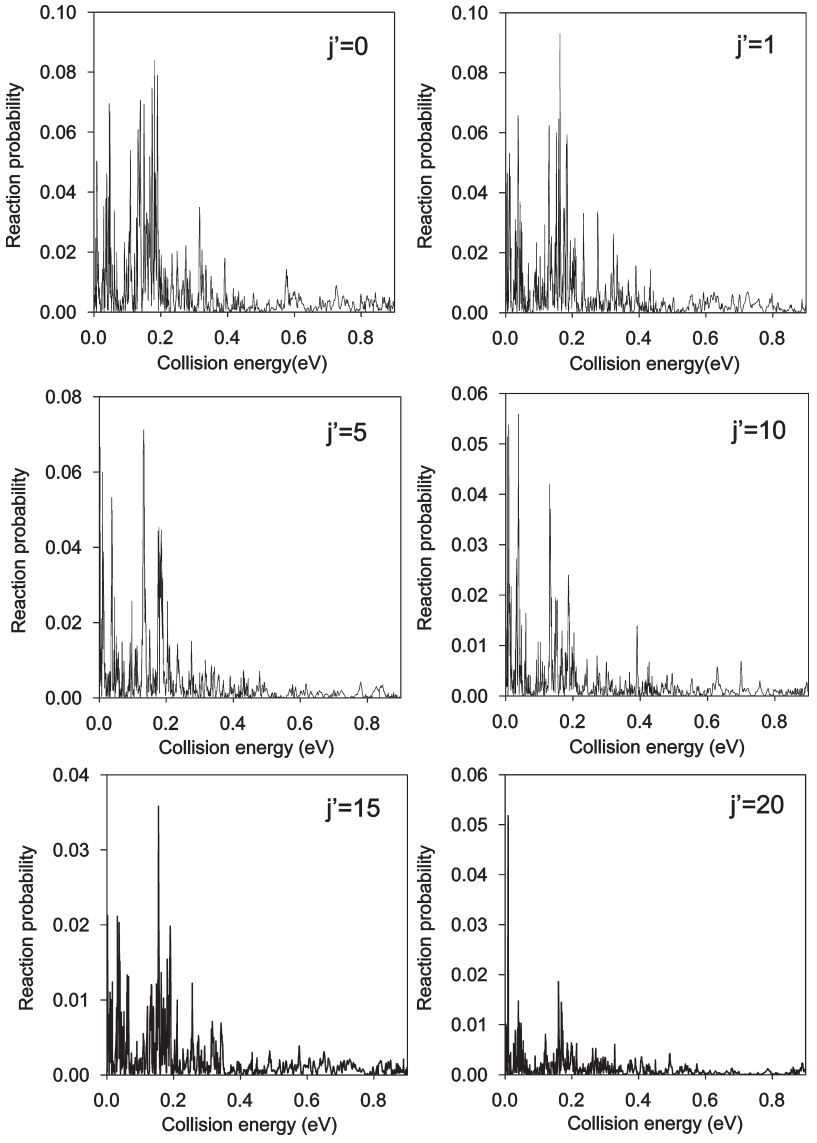

Figure 4. Rotationally state-resolved probabilities as a function of the collision energy for the C + OH($v = 0, j = 0$) → CO($a^3\Pi$)($v' = 0, j'$) + H reaction at $J = 0$.

for $J = 0$, and an approximate rate constant has been determined using a standard J-shifting method.

II. QUANTUM-MECHANICAL METHOD

Three-dimensional QM scattering calculations on the second excited $1^4A''$ PES for the C(^{3}P) + OH($X^2\Pi$) → CO($a^3\Pi$) + H(^{2}S) reaction have been performed at $J = 0$ using an accurate TIQM method.[9] This method based on body-frame democratic hyperspherical coordinates has already proved successful in describing complex-forming reactions, such as the OH + O,[10] OH + N,[11] and OH + S[13] reactions.

At each hyperradius ρ, we determined a set of eigenfunctions of a reference Hamiltonian $H_0 = T + V$, which incorporates the total energy with the kinetic energy T arising from deformation and rotation around the axis of least inertia and the potential energy V. At small ρ, the adiabatic states in each sector span a large fraction of configuration space and allow for atom exchange. These states are expanded on a basis of pseudo-hyperspherical harmonics. For total angular momentum $J = 0$, the scattering wave function is expanded on the basis of 720 states dissociating at large ρ into the OH(23,18,13), CO(92,87,82,76,70,63,56,47,37,23), and CH(14,4) rovibrational sets (this notation indicates the largest rotational level j for each vibrational manifold $v = 0-2$ for OH, $v = 0-9$ for CO, and $v = 0,1$ for CH). The CH + O channel is always closed for the 0−0.9 eV collision energy range considered in the present work. The coefficients of the expansion satisfy a set of second-order coupled differential equations with couplings arising from the difference between the exact Hamiltonian and the reference Hamiltonian. These coupled equations are solved using the Johnson−Manolopoulos log-derivative propagator.[14] Propagation goes from $\rho = 2.9$ to 21.1 a_0, including a total of 147 sectors into which the hyperradius ρ has been divided.

III. RESULTS AND DISCUSSION

Total reaction probability for the C(^{3}P) + OH($X^2\Pi$) → CO($a^3\Pi$) + H(^{2}S) reaction at $J = 0$ is shown in Figure 2 for

dx.doi.org/10.1021/jp202879n |J. Phys. Chem. A 2011, 115, 8791–8796

collision energies up to 0.9 eV. The energy step is 0.0005 eV over the whole energy range. No energy threshold is observed as expected for a barrierless reaction. The reaction probability is high at very low energy (0.87 at 0.009 eV), while above 0.2 eV it is much smaller. At the highest collision energies, the reactivity is reduced with a reaction probability less than 0.1, the back-dissociation processes[15] being dominant. This behavior is similar to that found on the $1^2A''$ PES, but it is in contrast with the result on the ground PES for which the reaction probability is near unity at all collision energies.[6]

The overall shape of the total TIQM reaction probability is well reproduced by the QCT prediction. The QCT reaction probability was computed for a zero impact parameter ($b = 0$) and OH($v = 0, j = 0$). However, the QCT result does not give any resonances because their origin is purely quantum. They are associated with the deep HCO/COH wells in the PES, which lead to quasibound states. In addition, the rising in TIQM reaction probability between 0.1 and 0.2 eV is not observed in the QCT calculations. Finally, the QCT reaction probability is slightly larger than the QM one above 0.2 eV. A similar degree of agreement between the TIQM and QCT results has been found with the $1^2A''$ PES. On the contrary, an excellent accord has been seen for the C + OH reaction on the ground PES,[6] where no resonances are found and the total reaction probability is very close to unity.

Similarly to the $1^2A''$ case, an extremely dense resonance structure is thus present in the total reaction probability, especially at low collision energy where some peaks are very intense and sharp. Interestingly, no resonances were found[6] on the ground PES in spite of a deeper well (−7.3 eV relative to the entrance channel), because the exoergicity for $C(^3P) + OH(X^2\Pi) \rightarrow CO(X^1\Sigma^+) + H(^2S)$ is much larger than that of the present reaction.

QM resonances in neutral−neutral reactions are usually associated with a deep well (typically several electron-volts) that supports a large number of bound states and gives rise to the formation of a long-lived intermediate complex with a lifetime that can be longer than its rotational period. However, the resonance peaks are very intense and sharp if the exoergicity is small. By contrast, higher exoergic reactions yield a faster decay and broader resonance widths.[11,16−20] In the exothermic C + OH → CO($a^3\Pi$) + H reaction through the $1^2A''$ PES characterized by two deep wells (COH: 4.6 eV relative to the entrance channel; HCO: 6.2 eV relative to the entrance channel) and a small exoergicity of −0.41 eV, a dense resonance structure was found, and the average lifetime of the resonant states of COH/HCO are long-lived (more than 1 ps).[12] This is in strong contrast with the C + OH → CO($X^1\Sigma^+$) + H reaction, which involves deeper wells (COH: 5.5 eV relative to the entrance channel; HCO: 7.3 eV relative to the entrance channel) but a much larger exoergicity (6.5 eV), yielding reaction probabilities with no resonances, which is almost unity in the presently considered energy range. The C + OH → CO($a^3\Pi$) + H reaction through the $1^4A''$ PES has the same exoergicity as that for the $1^2A''$ PES and also presents two deep wells (COH: 1.85 eV relative to the entrance channel; HCO: 2.25 eV relative to the entrance channel). So resonances are also found in the reaction probability computed using the $1^4A''$ PES. The very small exoergicity of barrierless reactions involving a deep well (or more) thus appears as an essential feature to obtain narrow resonances.

The vibrationally state-resolved reaction probabilities are displayed in Figure 3. Of course, a dense resonance structure is found too. However, they present some differences from the total reaction probability. For the vibrational state $v' = 0$ of the CO($a^3\Pi$) product, the shape of the reaction probability is close to that of the total reaction probability, and the magnitude is nearly the same. For $v' = 1$, the reaction probability is smaller (<0.15). For $v' = 2$, the reaction probability is even much smaller at very low collision energies, but there is no real energy threshold because the CO($a^3\Pi, v' = 2$) + H(^2S) channel lies 0.127 eV below the entrance channel. Above 0.15 eV, the $v' = 2$ reaction probability is, on average, almost constant around 0.01, except near 0.33 eV, where it reaches its maximum value of 0.054. The $v' = 3$ reaction probabilities present an energy threshold because the CO($a^3\Pi, v' = 3$) + H(^2S) channel becomes energetically accessible above 0.071 eV. The $v' = 3$ probability increases on average as the collision energy increases. The vibrationally state-resolved reaction probabilities therefore have different magnitudes for all v', and the $v' = 0$ reaction probability is dominant in the considered energy range.

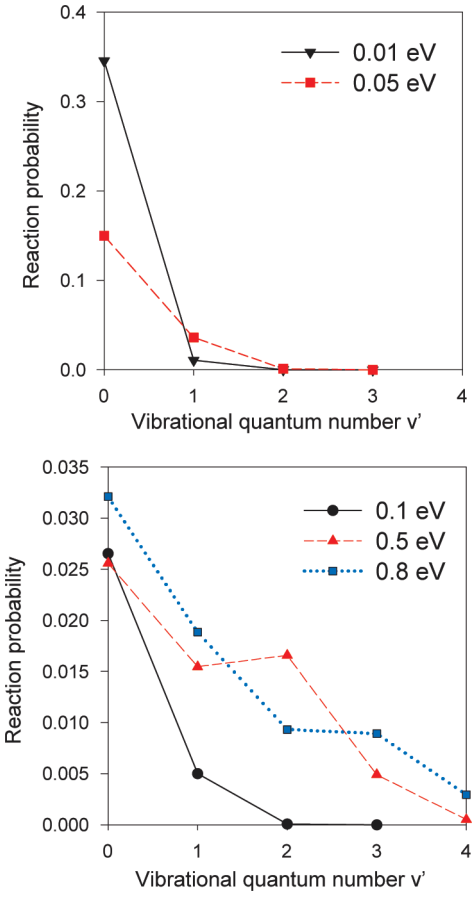

Figure 5. Product vibrational distributions at $J = 0$: vibrationally state-resolved reaction probabilities as a function of vibrational quantum number v' of CO($a^3\Pi$) at 0.01 and 0.05 (upper panel) and 0.1 and 0.5 eV (lower panel).

Figure 4 shows some rotationally state-resolved reaction probabilities for CO($a^3\Pi$)($v' = 0$) as a function of collision energy. The shapes and magnitudes are similar for $j' = 0$, 1, 5, 10, 15. For all j', the probability quickly varies with respect to the collision energy, showing a strong effect of the collision energy on the reactivity at the state-to-state level. At some collision energies, the reaction probability is almost zero, while at other

dx.doi.org/10.1021/jp202879n |J. Phys. Chem. A 2011, 115, 8791–8796

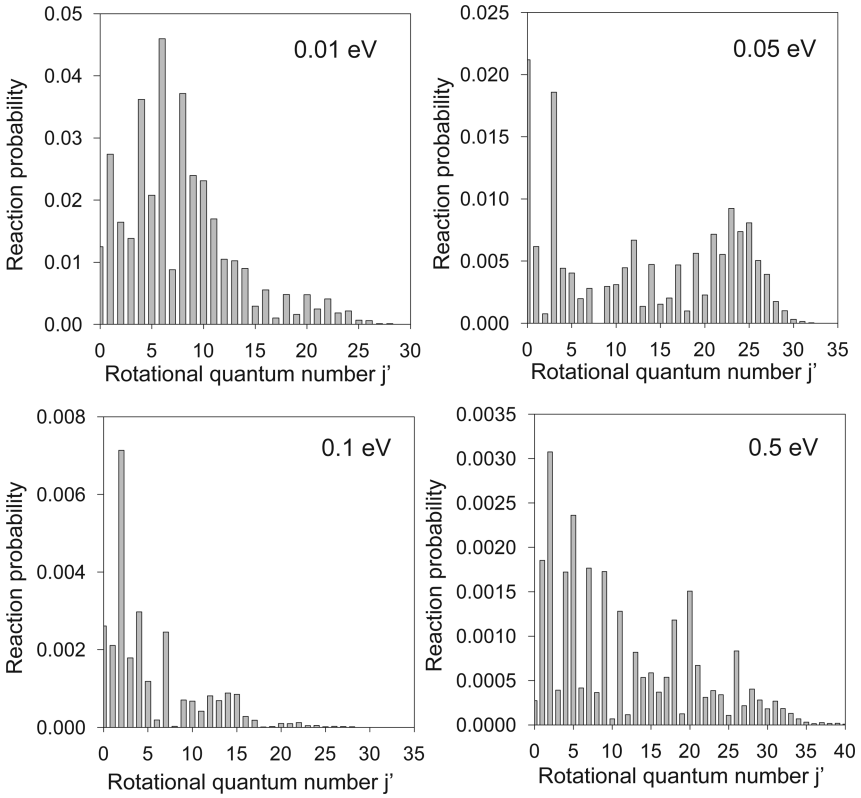

Figure 6. Product rotational distributions at $J = 0$: rotationally state-resolved reaction probabilities as a function of rotational quantum number j' of $CO(a^3\Pi)(v' = 0)$ at 0.01, 0.05, 0.1, and 0.5 eV.

energies (near the previous ones) it is non-negligible. The rotationally state-resolved reaction probabilities globally behave as the total reaction probability, with many pronounced resonances at low collision energy and broader small resonances at higher energy. Similar features were obtained on the $1^2A''$ PES.[8]

We have also computed the product vibrational and rotational distributions at five collision energies: 0.01, 0.05, 0.1, 0.5 and 0.8 eV. Figure 5 shows the vibrational distributions (reaction probability at $J = 0$ as a function of the $CO(a^3\Pi)$ vibrational quantum number v'), while Figure 6 displays the rotational distributions (reaction probability at $J = 0$ as a function of the $CO(a^3\Pi)$ rotational quantum number j') for $v' = 0$. As can be seen in Figure 5, at all collision energies (except at 0.5 eV where $v' = 2$ is slightly more populated than $v' = 1$), the reaction probability decreases as v' increases, showing a noninverted distribution. The vibrational distributions are therefore rather statistical. This result confirms that the reaction proceeds via the HCO/COH long-lived intermediate complexes and that the direct mechanism is not dominant. The situation is different from that found for C + OH on the ground PES (strong vibrational population inversion related to a direct mechanism[3,6]) and on the $1^2A''$ PES (both inverted and statistical distributions depending on the collision energy).

Concerning the rotational distributions (Figure 6), the reaction probability strongly depends on j' at each collision energy. All accessible rotational states are not populated (for instance, the probability is nearly zero at 0.05 eV for $j' = 8$), whereas only a few rotational states are highly populated ($j' = 0$ and $j' = 3$ at 0.05 eV). The distributions are rotationally cold, except at 0.05 eV where high j' are also populated. This result differs from

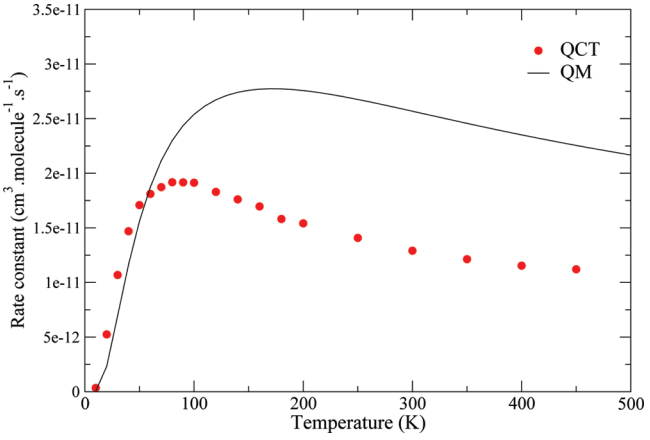

Figure 7. QM (solid line) and QCT (circles) rate constants for the C + $OH(v = 0, j = 0) \rightarrow CO(a^3\Pi)$ + H reaction. The QM rate constant has been obtained using the J-shifting approximation.

that obtained on the $1^2A''$ PES where the reaction probabilities have similar values for small, medium, and high j'.

We have also computed the QM rate constant for the ($v = 0$, $j = 0$) state of OH in the 10−500 K temperature range. The exact TIQM total reaction probability for $J = 0$ has been used, whereas for $J > 0$ a J-shifting approach[21] has been employed. Figure 7 shows the QM rate constant including the temperature-dependent electronic factor[22] as a function of temperature. The reaction is fast in a wide temperature range, and the rate constant has the usual dependence on temperature, as already found in the O + OH,[23,24] S + OH,[13] and N + NO[20] reactions. In the present

dx.doi.org/10.1021/jp202879n |J. Phys. Chem. A 2011, 115, 8791–8796

case, the rate constant sharply increases with temperature up to a maximum value of 2.80×10^{-11} cm^3 s^{-1} at 170 K, and then slowly decreases as the temperature increases. Such behavior (an increase, then a maximum, and finally a decrease with temperature) is characteristic of barrierless reactions when we include the spin−orbit structure of reactants through a temperature-dependent factor (as in the present study). These features can be found (in QM and QCT calculations) at low temperatures for barrierless-like integral cross sections (or reaction probabilities), as in the present case.

The QCT result is shown for comparison. The QCT calculations are obtained without the J-shifting approximation. The method employed here for OH($v = 0$, $j = 0$) is based on the trajectory framework and uses a direct sampling of the initial translational energies from the Maxwell−Boltzmann distribution. It is clear that the QCT method predicts a rate constant similar to the TIQM one for temperature below 60 K. However, a disagreement is observed above this temperature with a large underestimate of the QCT calculation. In addition, although the qualitative temperature dependence is well reproduced, the maximum value of the QCT rate constant is lower and located at around 85 K. Such differences have also been found in the O + OH reaction.[24] The better agreement observed between the QCT and TIQM/J-shifting results at low temperatures in comparison with the higher ones is rather surprising, as quantum effects are expected to be less important as temperature increases. This could be explained by the use of the J-shifting approximation in the TIQM calculation, which might not be accurate in predicting the reaction rate constant. Another reason for this discrepancy may be directly linked to the QCT method, which is based on classical mechanics. By nature, no quantum effect can occur, and, for example, the zero-point energy is not rigorously accounted for. In order to clarify the discrepancy between the QCT and TIQM/J-shifting rate constant, it is necessary to calculate an accurate thermal rate constant using, for instance, a TIQM method without dynamic approximations. Work in this direction is currently under way in our group.

IV. CONCLUSIONS

In this paper, we have reported accurate TIQM calculations performed on the second excited electronic state of $1^4A''$ symmetry for the $C(^3P) + OH(X^2\Pi) \rightarrow CO(a^3\Pi) + H(^2S)$ reaction using the ab initio PES built by our group.[4] Total and state-to-state reaction probabilities at $J = 0$ have been determined for the first time in the 0−0.9 eV energy range. The reaction probabilities as a function of the collision energy show a dense resonance structure, especially at low energy, due to long-lived resonances supported by the HCO/COH potential wells. The total reaction probability presents no energy threshold as expected for a barrierless reaction. We have found statistical product vibrational distributions, which is consistent with an indirect mechanism involving the long-lived HCO/COH intermediate complexes. The product rotational distributions are rather cold and are very specific in j'. The results reported here have been compared with those obtained on the ground PES and on the first excited state of $1^2A''$ symmetry and are often in contrast with them, because of different reaction mechanisms. The rate constant for C + OH($v = 0$, $j = 0$) has also been computed in the 10−500 K temperature range. We use the exact $J = 0$ total reaction probability and a J-shifting method for $J > 0$. The QCT prediction is in disagreement with the QM rate constant. It is worthwhile to recall that the QCT method neglects quantum effects and does not rigorously take into account the zero-point energy because it is based on classical mechanics.

Finally, an accurate QM calculation including all the partial waves J will be the big next step. This should allow the first determination of converged integral and differential cross sections and an accurate rate constant for the title reaction.

■ ACKNOWLEDGMENT

The computations were performed on the machine of the Mésocentre de calcul de Franche-Comté.

■ REFERENCES

(1) Zanchet, A.; Bussery-Honvault, B.; Honvault, P. *J. Phys. Chem. A* **2006**, *110*, 12017.
(2) Zanchet, A.; Halvick, P.; Rayez, J.-C.; Bussery-Honvault, B.; Honvault, P. *J. Chem. Phys.* **2007**, *126*, 184308.
(3) Zanchet, A.; Halvick, P.; Bussery-Honvault, B.; Honvault, P. *J. Chem. Phys.* **2008**, *128*, 204301.
(4) Zanchet, A.; Bussery-Honvault, B.; Jorfi, M.; Honvault, P. *Phys. Chem. Chem. Phys.* **2009**, *11*, 6182.
(5) Lin, S. Y.; Guo, H.; Honvault, P. *Chem. Phys. Lett.* **2008**, *453*, 140.
(6) Bulut, N.; Zanchet, A.; Honvault, P.; Bussery-Honvault, B.; Banares, L. *J. Chem. Phys.* **2009**, *130*, 194303.
(7) Ho, T.-S.; Hollebeck, T.; Rabitz, H.; Harding, L. B.; Schatz, G. C. *J. Chem. Phys.* **1996**, *105*, 10472.
(8) Jorfi, M; Honvault, P *J. Phys. Chem. A* **2010**, *114*, 4742.
(9) Honvault, P.; Launay, J.-M. *Theory of Chemical Reaction Dynamics*; Lagana, A., Lendvay, G., Eds.; Kluwer: Dordrecht, The Netherlands, 2004; p 187.
(10) Lin, S. Y.; Guo, H.; Honvault, P.; Xu, C.; Xie, D. *J. Chem. Phys.* **2008**, *128*, 014303.
(11) Jorfi, M.; Honvault, P. *J. Phys. Chem. A* **2009**, *113*, 2316.
(12) Jorfi, M.; Honvault, P.; Zanchet, A.; Bussery-Honvault, B., in preparation.
(13) Jorfi, M; Honvault, P *J. Chem. Phys.* **2010**, *133*, 144315.
(14) Manolopoulos, D. E. *J. Chem. Phys.* **1986**, *85*, 6425.
(15) Jorfi, M.; Honvault, P.; Bargueno, P.; González-Lezana, T.; Larrégaray, P.; Bonnet, L.; Halvick, P. *J. Chem. Phys.* **2009**, *130*, 184301.
(16) Rackham, E. J.; González-Lezana, T.; Manolopoulos, D. E. *J. Chem. Phys.* **2003**, *119*, 12895.
(17) Banares, L.; Aoiz, F. J.; Honvault, P.; Bussery-Honvault, B.; Launay, J.-M. *J. Chem. Phys.* **2003**, *118*, 565.
(18) Banares, L.; Castillo, J. F.; Honvault, P.; Launay, J.-M. *Phys. Chem. Chem. Phys.* **2005**, *7*, 627.
(19) Jorfi, M.; Honvault, P.; Halvick, P.; Lin, S. Y.; Guo, H. *Chem. Phys. Lett.* **2008**, *462*, 53.
(20) Jorfi, M.; Honvault, P. *J. Phys. Chem. A* **2009**, *113*, 10648.
(21) Bowman, J. M. *J. Phys. Chem.* **1991**, *95*, 4960.
(22) Graff, M. M.; Wagner, A. F. *J. Chem. Phys.* **1990**, *92*, 2423.
(23) Xu, C.; Xie, D.; Honvault, P.; Lin, S. Y.; Guo, H. *J. Chem. Phys.* **2007**, *127*, 024304.
(24) Lique, F.; Jorfi, M.; Honvault, P.; Halvick, P.; Lin, S. Y.; Guo, H.; Xie, D.; Klos, J.; Dagdigian, P. J.; Alexander, M. H. *J. Chem. Phys.* **2009**, *131*, 221104.